Technical Brief

MALDI mass spectrometry imaging of *N*-glycans on tibial cartilage and subchondral bone proteins in knee osteoarthritis

Matthew T. Briggs[1,2], Julia S. Kuliwaba[3,4], Dzenita Muratovic[3,4], Arun V. Everest-Dass[5,6], Nicolle H. Packer[5,6], David M. Findlay[3], Peter Hoffmann[1,2].

(1) Adelaide Proteomics Centre, School of Biological Sciences, University of Adelaide, Adelaide, South Australia, 5005, Australia.
(2) Institute of Photonics and Advanced Sensing (IPAS), University of Adelaide, Adelaide, South Australia, 5005, Australia.
(3) Discipline of Orthopaedics and Trauma, School of Medicine, University of Adelaide, Adelaide, South Australia, 5005, Australia.
(4) Bone and Joint Research Laboratory, SA Pathology, Adelaide, South Australia, 5000, Australia.
(5) Biomolecular Frontiers Research Centre, Faculty of Science, Macquarie University, Sydney, New South Wales, 2109, Australia.
(6) Centre of Excellence for Nanoscale BioPhotonics (CNBP), University of Adelaide, Adelaide, South Australia, 5005, Australia.

To whom all correspondence and requests for reprints should be addressed:
Prof. Peter Hoffmann,
Adelaide Proteomics Centre, School of Molecular and Biomedical Science, University of Adelaide, Adelaide, South Australia 5005.
Phone: +61 (08) 8313 5507; Fax: +61 (08) 0 8313 4362;
Email: peter.hoffmann@adelaide.edu.au

Received: 18-11-2015; Revised: 15-02-2016; Accepted: 11-03-2016

This article has been accepted for publication and undergone full peer review but has not been through the copyediting, typesetting, pagination and proofreading process, which may lead to differences between this version and the Version of Record. Please cite this article as doi: 10.1002/pmic.201500461.

Abbreviations: Osteoarthritis (OA), bone marrow lesion (BML), magnetic resonance imaging (MRI), extracellular matrix (ECM), formalin-fixed paraffin-embedded (FFPE), proton density-weighted (PDFS), indium tin oxide (ITO), polyethylene naphthalate (PEN), citric acid antigen retrieval (CAAR).

Keywords: bone marrow lesion, glycans, maldi imaging, mass spectrometry, osteoarthritis

Words (including references as well as figure and table legends): 3,034

Abstract:

Magnetic Resonance Imaging (MRI) is a non-invasive technique routinely used to investigate pathological changes in knee osteoarthritis (OA) patients. MRI uniquely reveals zones of the most severe change in the subchondral bone (SCB) in OA, called bone marrow lesions (BMLs). BMLs have diagnostic and prognostic significance in OA, but MRI does not provide a molecular understanding of BMLs. Multiple *N*-glycan structures have been observed to play a pivotal role in the OA disease process. We applied matrix-assisted laser desorption/ionization (MALDI) mass spectrometry imaging (MSI) of *N*-glycans to formalin-fixed paraffin-embedded (FFPE) SCB tissue sections from patients with knee OA, and liquid chromatography-electrospray ionization-tandem mass spectrometry (LC-ESI-MS/MS) was conducted on consecutive sections to structurally characterize and correlate with the *N*-glycans seen by MALDI-MSI. The application of this novel MALDI-MSI protocol has enabled the first steps to spatially investigate the *N*-glycome in the SCB of knee OA patients.

Human osteoarthritis (OA) is an increasingly prevalent age-related joint disease with a high burden of personal and economic cost. The disease is characterized by articular cartilage degeneration, with the addition of both generalized and focal changes of the subchondral bone [1, 2]. Bone marrow lesions (BMLs) are features that have been identified in both early asymptomatic and severe late-stage OA patients and their presence associates with loss of overlying cartilage [3, 4]. Classically, BMLs are identified using magnetic resonance imaging (MRI) by either fat-suppressed and/or proton dense T2 weighted scans. The difference between T1 and T2 weighted scans is that BML areas appear hypointense (i.e. low signal) for T1 and hyperintense (i.e. high signal) for T2 [5, 6]. Therefore, T2 weighted scans depict BMLs to their full extent, while T1 weighted scans usually assess cartilage. A combination of these sequences provides diagnostic and prognostic information regarding OA disease progression [7, 8]. However, MRI does not provide a molecular understanding of BML formation and OA disease progression.

Adjacent to BMLs in the SCB is overlying cartilage composed of extracellular matrix (ECM) glycoproteins [9, 10]. Besides proteoglycans, there are glycosylated cell surface proteins, such as

CD44 and integrins, which play an important role in mediating chondrocyte and ECM interactions [11, 12]. Glycans attached to these cartilage ECM glycoproteins are classified into two groups: (i) *N*-linked glycans that are attached to asparagine residues and (ii) *O*-linked glycans that are attached to serine/threonine residues [13]. *N*-glycans are the most common glycan, with well-established methods for analysis from tissue [14, 15]. Multiple *N*-glycan structures have been observed to play a pivotal role in OA disease progression. Recently, using high-performance liquid chromatography (HPLC) mass spectrometry (MS), it has been shown that high-mannose type *N*-glycans are significantly decreased on proteins in tissue from both murine and human OA cartilage [16]. In 2013, glycophenotyping of OA cartilage was carried out using several techniques, such as RT-PCR, mass spectrometry and immunohistochemistry. Liquid chromatography-electrospray ionization-tandem mass spectrometry (LC-ESI-MS/MS) separation and structural identification of the released glycans confirmed 21 *N*-glycans on the human OA chondrocyte proteins isolated from femoral condyle articular cartilage [17]. The *N*-glycome of bone marrow from OA patients has not yet been characterized.

MALDI mass spectrometry imaging (MALDI-MSI) has previously been applied to the proteomic analysis of fresh frozen human OA knee cartilage and synovial tissue. Deep and superficial knee cartilage from human healthy and OA patients were sectioned and analyzed by MALDI-MSI of the tryptic peptides [18]. Fibronectin and cartilage oligomeric matrix protein (COMP) were 2 glycoproteins identified in the OA patients, but not in the healthy controls. Moreover, the glycoprotein fibronectin was identified in the synovial membranes from OA patients, but not in healthy controls. In summary, glycoproteins have been observed to play an important role in OA changes of human knee cartilage and synovial tissue.

The measurement of *N*-glycans by MALDI-MSI on fresh frozen mouse brain tissue and various formalin-fixed paraffin-embedded (FFPE) tissues has been established previously [19, 20], with regions of interest, such as tumour and non-tumour, differentiated based on the pattern of *N*-glycans released. The limitation of MALDI analysis is that *N*-glycan masses can identify the glycan compositions but cannot identify the sequence and branching of the glycan structures. This has recently been overcome with a new workflow combining *N*-glycan analysis by MALDI-MSI and LC-ESI-MS/MS [21].

Here we investigate the *N*-glycome of FFPE cartilage and bone marrow tissue. Human knee SCB, from OA patients with BMLs (stage 1 and 2) or without BMLs were analysed to investigate *N*-glycosylation patterns.

Tibial plateaus were obtained from three patients (one male aged 52 years, two females aged 68 and 74 years) undergoing knee arthroplasty surgery for radiographic and severe symptomatic OA. Tibial plateau specimens were scanned *ex vivo,* using an MR scanner with an 8-channel wrist coil (3T MRI Siemens TRIO), at two specific sequences; fat suppressed (FS) fast spin-echo proton density-weighted (PDFS) and T1 weighted spin echo in sagittal and coronal plane. Sagittal slice thickness was 1.6 mm with distance factor of 25%. Coronal slice thickness was 3.0 mm with 10% distance factor. *Ex vivo* MR imaging was confirmed to correspond to pre-operative imaging, by comparing pre- and post-operative MR data. BMLs were defined as changes of the MRI signal intensity in the bone marrow, located beneath cartilage and visible at least on 2 consecutive slices. BMLs detected on the PDFS sequence only (no signal on T1) are classified as BML stage 1 and correspond to mild-to-moderate osteochondral OA pathology; BMLs detected on both PDFS and T1 sequences are classified as BML stage 2 and represent severe OA osteochondral pathology [22]. Using precise mapping of BMLs (OsiriX software, Pixmeo-SARL, Switzerland), a sagittal slice of cartilage-subchondral bone (width 5mm x depth 5 to 12mm) containing the BML area (**Figure 1**) was dissected using a low speed diamond wheel saw (Model 660, South Bay Technology, Inc.). Sagittal blocks of tissue were fixed in 4% (w/v) paraformaldehyde and slowly decalcified in 15% (w/v) ethylenediaminetetra acetic acid (EDTA). Following complete decalcification as determined by X-ray, samples were processed, embedded in paraffin and cut on a rotary microtome (Leica RM 2235 Nussloch, Germany) into 5µm thick sections.

FFPE human OA tissue sections on indium tin oxide (ITO) or polyethylene naphthalate (PEN) slides were rehydrated using a modified procedure of citric acid antigen retrieval (CAAR) at 70° for 3 h instead of 98° for 30 min and printing 15 nL of PNGase F instead of printing 30 nL of PNGase F [21]. Mass spectra were acquired using an ultrafleXtreme MALDI-TOF/TOF mass spectrometer or LC-iontrap ESI-MS/MS analysis as described previously [21, 23].

Bone marrow lesions (BMLs) were identified using PDFS and T1 weighted scans in magnetic resonance imaging (MRI) of the tibial plateaus. As depicted in **Figure 1 Panel a**, there was no BML detected in this patient, while in **Figure 1 Panels b and c**, BML stage 1 and 2, respectively, were detected. These BMLs are annotated in pink and green, as indicated on the MRI. Below each MRI are shown stained formalin-fixed paraffin-embedded (FFPE) tissue sections. Haematoxylin and eosin (H&E) staining provides histological information and safranin-O highlights the cartilage in red. Following acquisition of the MRI, the image was overlaid with the stained FFPE tissue sections and regions of no BML and BML stages 1 and 2 were annotated in black. Although the identification of these BMLs using MRI is useful, it does not provide molecular information. Therefore, we performed MALDI mass

spectrometry imaging (MALDI-MSI) of the released *N*-glycans to investigate the molecular mechanisms behind BMLs.

For the citric acid antigen retrieval (CAAR) [21, 24], we reduced the temperature and incubated longer to maintain adherence to the ITO slide. MALDI-MSI experiments were conducted in parallel with LC-ESI-MS/MS structural characterization. Consecutive tissue sections were manually micro-dissected, and the *N*-glycans were released and structurally characterized by LC-ESI-MS/MS. **Figure 2** represents the summed LC-ESI-MS and MALDI-MS profiles of both bone marrow and cartilage. In **Figure 2 Panel a** (LC-ESI-MS profiles), 52 individual *N*-glycan masses (including structural and compositional isomers) were identified from bone marrow proteins compared to 56 individual *N*-glycan masses (including structural and compositional isomers) identified from cartilage proteins, based on LC-ESI-MS/MS data **(Supplementary Table 1).** The detailed structures were manually assigned from the MS/MS fragmentation data as illustrated in **Supplementary Figure 1**. A comparison of the LC-ESI-MS mass profiles revealed differences in intensity of particular *m/z* values. For example, *m/z* 1111.4 was observed as a lower intensity peak in the cartilage relative to the bone marrow.

Ion intensity maps were then generated by MALDI-MSI for *N*-glycan structures from the complex/hybrid, sialylated and high-mannose families that had been determined by LC-ESI-MS/MS analysis (refer to **Figure 2 Panel a** for the summed LC-ESI-MS profiles). **Figure 3** shows safranin-O stained images and ion intensity maps for the same 3 patients described in **Figure 1**. The region annotated in black represents the control (i.e. non-treated) and calibrant regions while the region annotated in white is cartilage. There were no differences observed between the complex/hybrid *N*-glycan masses in both the cartilage and bone marrow (even between fucosylated and non-fucosylated *N*-glycans). The log ion intensity map for $(HexNAc)_2(Man)_3$ + $(Hex)_2(HexNAc)_2(NeuAc)_1$ was observed as a doubly sodiated species only in the cartilage whereas the core fucosylated version of this *N*-glycan was observed in both the cartilage and bone marrow. In addition, $(HexNAc)_2(Man)_3$ + $(Hex)_2(HexNAc)_2(NeuAc)_2$ was observed as a triply sodiated species only in the bone marrow of the patient with BML stage 1, but not in patients without BML or BML stage 2 as classified by MRI. This particular *N*-glycan was observed in LC-ESI-MS/MS profiles of both the cartilage and bone marrow, but exhibited decreased intensity in cartilage. This suggests that this *N*-glycan is too low in abundance in the cartilage for MALDI-MSI detection. High mannose *N*-glycans such as $(HexNAc)_2(Man)_3$ + $(Hex)_3$, $(HexNAc)_2(Man)_3$ + $(Hex)_4$ and $(HexNAc)_2(Man)_3$ + $(Hex)_5$ were compared between the three knee OA patients. The ion intensity map for $(HexNAc)_2(Man)_3$ + $(Hex)_3$ showed that this *N*-glycan was only observed in the cartilage region,

whereas $(HexNAc)_2(Man)_3$ + $(Hex)_4$ and $(HexNAc)_2(Man)_3$ + $(Hex)_5$ are highlighted in both the cartilage and bone marrow.

Regions of interest (i.e. bone marrow and cartilage) were also selected based on histology and summed spectra were extracted from the MALDI-MSI dataset. **Figure 2 panel b** represents summed spectra from these regions and show a lower sensitivity of detection compared to LC-ESI-MS/MS. A comparison of those structures found by MALDI-MSI and LC-ESI-MS/MS are shown in **Supplementary Table 1**. The detected *m/z* from LC-ESI-MS corresponded to doubly charged $[M-2H]^{2-}$ masses and the *m/z* from MALDI–MSI corresponded to the sodiated mass ($[M+Na^+]^+$. A total of 17 individual *N*-glycan masses were identified from bone marrow compared to 20 individual *N*-glycan masses from cartilage. As previously seen in the ion intensity maps, $(HexNAc)_2(Man)_3$ + $(Hex)_2(HexNAc)_2(NeuAc)_1$ was only detected in the cartilage while $(HexNAc)_2(Man)_3$ + $(Hex)_2(HexNAc)_2(NeuAc)_2$ was only detected in the bone marrow. There was a major difference between the intensity of the *N*-glycan *m/z* values observed with $(HexNAc)_2(Man)_3$ + $(Hex)_3$ being prominent in the cartilage relative to the bone marrow.

In summary, we have established a MALDI-MSI and LC-ESI-MS/MS workflow for FFPE tibial cartilage and SCB of knee OA patients. For the first time, the *N*-glycome of different regions of the same OA sample have been investigated, with individual *N*-glycan structural and compositional isomers in bone marrow and cartilage (a total of 52 and 56 respectively) being identified by LC-ESI-MS/MS. Using targeted masses in the MALDI-MSI experiments, the disialylated biantennary complex glycan, $(HexNAc)_2(Man)_3$ + $(Hex)_2(HexNAc)_2(NeuAc)_2$ was identified to be prominent in the bone marrow for the BML stage 1 patient relative to all other patient samples. However, larger patient studies will be required in order to understand the biological relevance of this observation. Overall, further development of this novel MALDI-MSI protocol has enabled the first steps to investigate the spatial distribution of the *N*-glycome of knee OA patients.

Figure 1: Knee osteoarthritis (OA) patients (a) without bone marrow lesions (No BML), (b) with BML stage 1 (BML 1), and (c) with BML stage 2 (BML 2). Each panel includes (from top to bottom) a PDFS-weighted MRI of the tibial plateau (BML stage 1 and 2 are annotated in pink and green, respectively), a haematoxylin and eosin (H&E) stain, and a Safranin-O/Fast Green stain of consecutive FFPE tissue sections. Regions of interest are annotated in black.

Figure 2: (a) LC-ESI-MS profiles of bone marrow and cartilage regions, and (b) MALDI-MS profiles of bone marrow and cartilage regions, annotated with confirmed *N*-glycan structures from LC-ESI-MS/MS. (a) *N*-glycans were released in-solution from formalin-fixed paraffin-embedded (FFPE) tissue sections using PNGase F prior to LC-ESI-MS/MS. (b) *N*-glycans were released *in situ* from FFPE tissue sections using PNGase F and analysed by MALDI-TOF/TOF-MS. Regions were selected based on histology in SCiLS lab software (V2015a, Bruker Daltonics, Bremen, Germany).

Figure 3: Safranin-O stained images and ion intensity maps of complex/hybrid, sialylated and high-mannose *N*-glycans observed in patients without bone marrow lesions (No BML), with BML stage 1 (BML 1) and with BML stage 2 (BML 2). *N*-glycans were released *in situ* on FFPE tissue sections using PNGase F and analyzed by MALDI-TOF/TOF-MS. *m/z* values were selected and visualized in SCiLS lab software (V2015a, Bruker Daltonics, Bremen, Germany). Ion intensity maps were co-registered with safranin-O stained images to identify the distribution of the selected *N*-glycans. There was no distinct pattern between the same families (i.e. complex/hybrid, sialylated and high-mannose) of N-glycans. Control and calibrant regions (i.e. regions not treated with PNGase F) are annotated in black.

Acknowledgements

P.H gratefully acknowledges the financial support of the Australian Research Council (ARC LP110100693), Bioplatforms Australia, and the Government of South Australia. NHP and AVE-D acknowledges the financial support of the ARC CoE in NanoScale BioPhotonics (ARC CE140100003)

Conflicts of interest

The authors have declared no conflict of interest.

References:

[1] Fautrel, B., Bourgeois, P., [Rheumatic disorders. Overview]. *Drugs* 2000, *59 Spec No 1*, 1-9.

[2] Beaupre, G. S., Stevens, S. S., Carter, D. R., Mechanobiology in the development, maintenance, and degeneration of articular cartilage. *Journal of rehabilitation research and development* 2000, *37*, 145-151.

[3] Roemer, F. W., Guermazi, A., Javaid, M. K., Lynch, J. A.*, et al.*, Change in MRI-detected subchondral bone marrow lesions is associated with cartilage loss: the MOST Study. A longitudinal multicentre study of knee osteoarthritis. *Annals of the rheumatic diseases* 2009, *68*, 1461-1465.

[4] Wluka, A. E., Hanna, F., Davies-Tuck, M., Wang, Y.*, et al.*, Bone marrow lesions predict increase in knee cartilage defects and loss of cartilage volume in middle-aged women without knee pain over 2 years. *Annals of the rheumatic diseases* 2009, *68*, 850-855.

[5] Loeuille, D., Chary-Valckenaere, I., MRI in OA: from cartilage to bone marrow lesion. *Osteoporosis international : a journal established as result of cooperation between the European Foundation for Osteoporosis and the National Osteoporosis Foundation of the USA* 2012, *23 Suppl 8*, S867-869.

[6] Dore, D., Martens, A., Quinn, S., Ding, C.*, et al.*, Bone marrow lesions predict site-specific cartilage defect development and volume loss: a prospective study in older adults. *Arthritis research & therapy* 2010, *12*, R222.

[7] Driban, J. B., Tassinari, A., Lo, G. H., Price, L. L.*, et al.*, Bone marrow lesions are associated with altered trabecular morphometry. *Osteoarthritis and cartilage / OARS, Osteoarthritis Research Society* 2012, *20*, 1519-1526.

[8] Hayashi, D., Guermazi, A., Kwoh, C. K., Hannon, M. J.*, et al.*, Semiquantitative assessment of subchondral bone marrow edema-like lesions and subchondral cysts of the knee at 3T MRI: a comparison between intermediate-weighted fat-suppressed spin echo and Dual Echo Steady State sequences. *BMC musculoskeletal disorders* 2011, *12*, 198.

[9] Toegel, S., Pabst, M., Wu, S. Q., Grass, J.*, et al.*, Phenotype-related differential alpha-2,6- or alpha-2,3-sialylation of glycoprotein N-glycans in human chondrocytes. *Osteoarthritis and cartilage / OARS, Osteoarthritis Research Society* 2010, *18*, 240-248.

[10] Ishihara, T., Kakiya, K., Takahashi, K., Miwa, H.*, et al.*, Discovery of novel differentiation markers in the early stage of chondrogenesis by glycoform-focused reverse proteomics and genomics. *Biochimica et biophysica acta* 2014, *1840*, 645-655.

[11] Knudson, C. B., Knudson, W., Cartilage proteoglycans. *Seminars in cell & developmental biology* 2001, *12*, 69-78.

[12] Nicoll, S. B., Barak, O., Csoka, A. B., Bhatnagar, R. S., Stern, R., Hyaluronidases and CD44 undergo differential modulation during chondrogenesis. *Biochemical and biophysical research communications* 2002, *292*, 819-825.

[13] Kobata, A., Structures and functions of the sugar chains of glycoproteins. *European journal of biochemistry / FEBS* 1992, *209*, 483-501.

[14] Tian, Y., Gurley, K., Meany, D. L., Kemp, C. J., Zhang, H., N-linked glycoproteomic analysis of formalin-fixed and paraffin-embedded tissues. *Journal of proteome research* 2009, *8*, 1657-1662.

[15] Hu, Y., Zhou, S., Khalil, S. I., Renteria, C. L., Mechref, Y., Glycomic profiling of tissue sections by LC-MS. *Analytical chemistry* 2013, *85*, 4074-4079.

[16] Urita, A., Matsuhashi, T., Onodera, T., Nakagawa, H.*, et al.*, Alterations of high-mannose type N-glycosylation in human and mouse osteoarthritis cartilage. *Arthritis and rheumatism* 2011, *63*, 3428-3438.

[17] Toegel, S., Bieder, D., Andre, S., Altmann, F.*, et al.*, Glycophenotyping of osteoarthritic cartilage and chondrocytes by RT-qPCR, mass spectrometry, histochemistry with

plant/human lectins and lectin localization with a glycoprotein. *Arthritis research & therapy* 2013, *15*, R147.

[18] Cillero-Pastor, B., Eijkel, G. B., Kiss, A., Blanco, F. J., Heeren, R. M., Matrix-assisted laser desorption ionization-imaging mass spectrometry: a new methodology to study human osteoarthritic cartilage. *Arthritis and rheumatism* 2013, *65*, 710-720.

[19] Powers, T. W., Jones, E. E., Betesh, L. R., Romano, P. R.*, et al.*, Matrix assisted laser desorption ionization imaging mass spectrometry workflow for spatial profiling analysis of N-linked glycan expression in tissues. *Analytical chemistry* 2013, *85*, 9799-9806.

[20] Powers, T. W., Neely, B. A., Shao, Y., Tang, H.*, et al.*, MALDI imaging mass spectrometry profiling of N-glycans in formalin-fixed paraffin embedded clinical tissue blocks and tissue microarrays. *PloS one* 2014, *9*, e106255.

[21] Gustafsson, O. J., Briggs, M. T., Condina, M. R., Winderbaum, L. J.*, et al.*, MALDI imaging mass spectrometry of N-linked glycans on formalin-fixed paraffin-embedded murine kidney. *Analytical and bioanalytical chemistry* 2015, *407*, 2127-2139.

[22] D. Muratovic, F. M. C., A.E. Wluka, Y. Wang, D.M. Findlay, S. Otto, D.J. Taylor, S. Collings, J.M. Humphries, Y.R. Lee, G. Mercer, J.S. Kuliwaba., Bone marrow lesions detected by different magnetic resonance sequences as potential biomarkers for knee osteoarthritis: Comprehensive tissue level analysis. . *Osteoarthritis and Cartilage* 2015, *23*, A303–A305.

[23] Jensen, P. H., Karlsson, N. G., Kolarich, D., Packer, N. H., Structural analysis of N- and O-glycans released from glycoproteins. *Nature protocols* 2012, *7*, 1299-1310.

[24] Gustafsson, J. O., Oehler, M. K., McColl, S. R., Hoffmann, P., Citric acid antigen retrieval (CAAR) for tryptic peptide imaging directly on archived formalin-fixed paraffin-embedded tissue. *Journal of proteome research* 2010, *9*, 4315-4328.

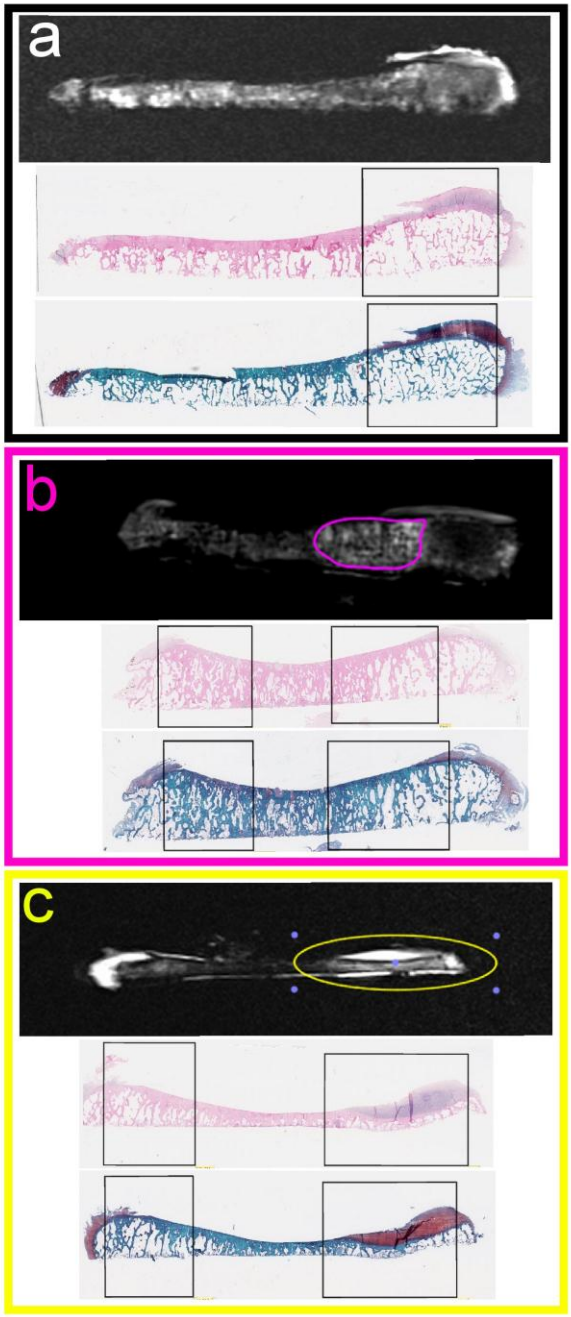

291

292

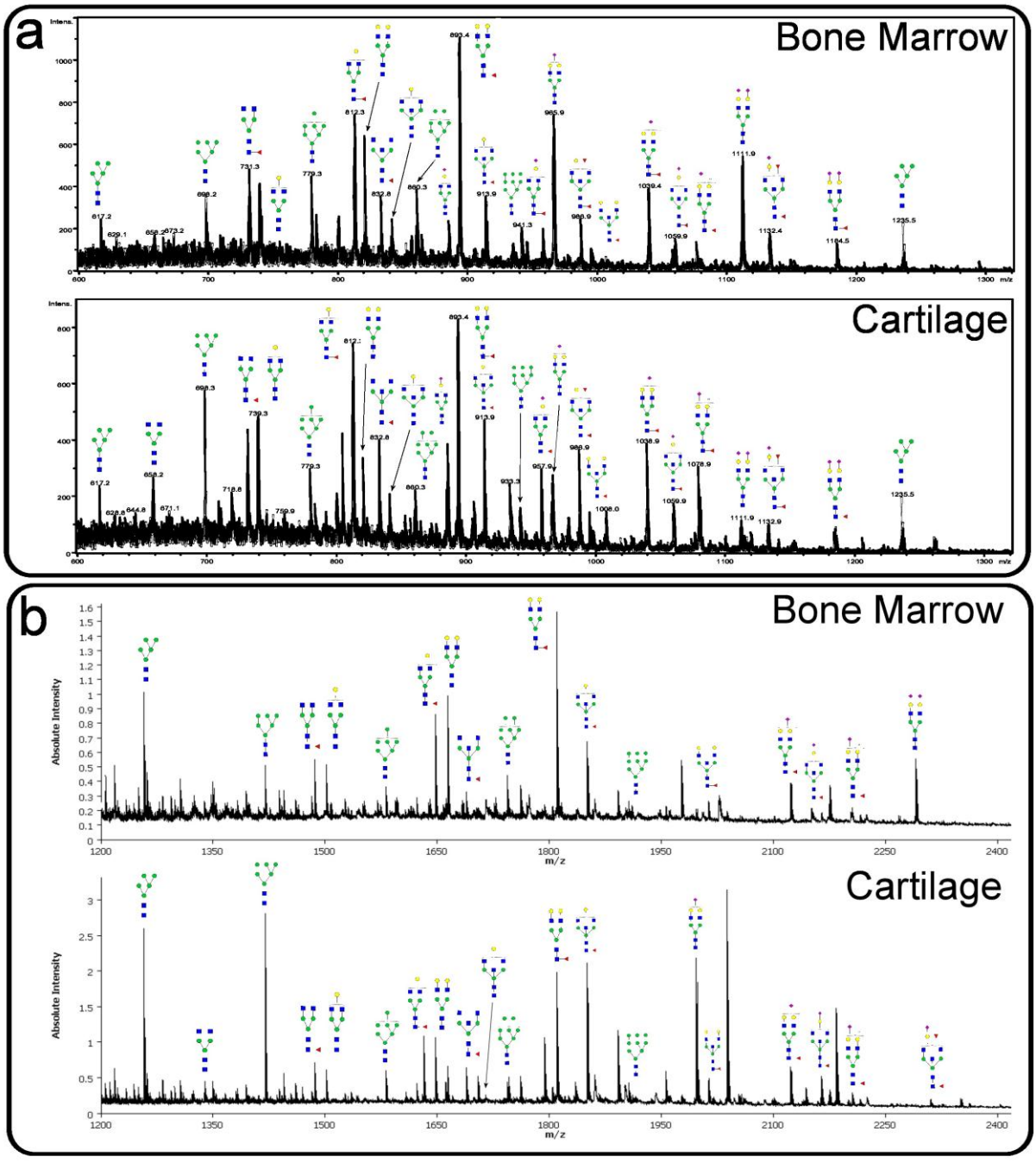

293

294

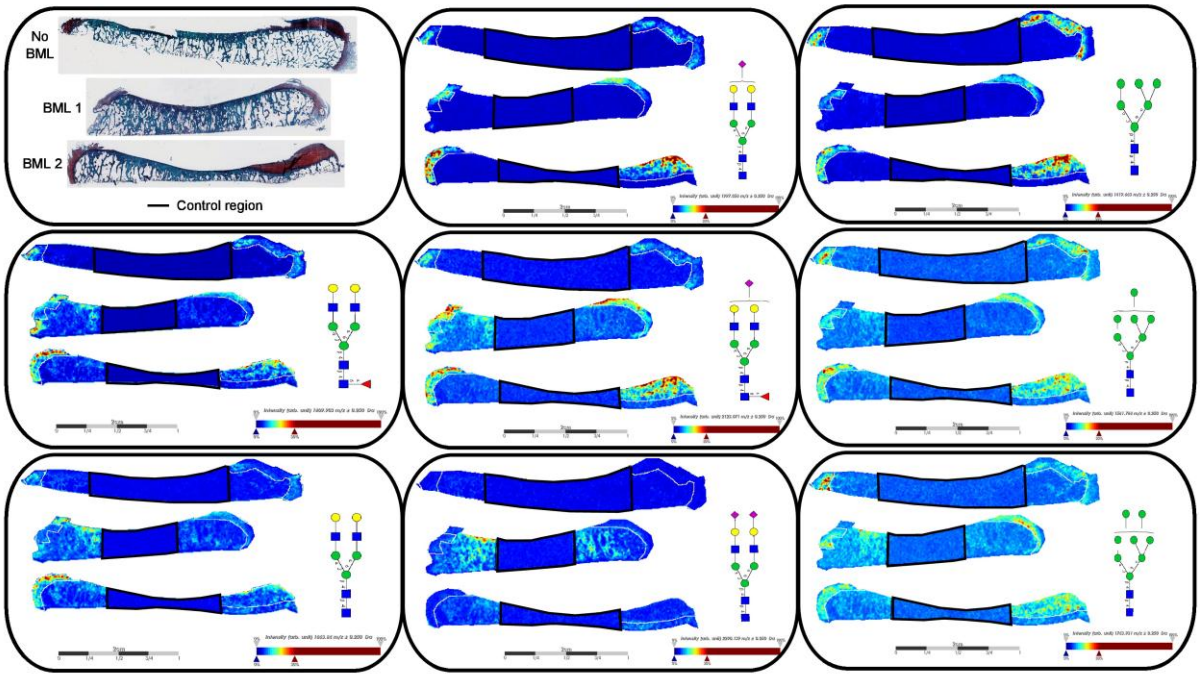

295

296